When VLT Meets HST: The HUGS Survey

Adriano Fontana[1]
Jim S. Dunlop[2]
Diego Paris[1]
Thomas Targett[2,3]
Konstantina Boutsia[1]
Marco Castellano[1]
Audrey Galametz[1]
Andrea Grazian[1]
Ross McLure[2]
Emiliano Merlin[1]
Laura Pentericci[1]
Styin Wuyts[4]
Omar Almaini[5]
Karina Caputi[6]
Ranga-Ram Chary[7]
Michele Cirasuolo[2]
Chris Conselice[5]
Ashanta Cooray[8]
Emanuele Daddi[9]
Mark Dickinson[10]
Sandra M. Faber[11]
Giovanni Fazio[12]
Henry Ferguson[13]
Emanuele Giallongo[1]
Mauro Giavalisco[14]
Norman Grogin[13]
Nimish Hathi[15]
Anton Koekemoer[13]
David C. Koo[11]
Ray Lucas[13]
Mario Nonino[16]
Hans-Walter Rix[17]
Alvio Renzini[18]
David Rosario[4]
Paola Santini[1]
Claudia Scarlata[19]
Veronica Sommariva[1,20]
Daniel P. Stark[21]
Arjien van der Wel[17]
Eros Vanzella[20]
Vivienne Wild[22,2]
Haojing Yan[23]
Stefano Zibetti[24]

[1] INAF–Osservatorio Astronomico di Roma, Monte Porzio Catone, Italy
[2] Institute for Astronomy, University of Edinburgh, Royal Observatory, Edinburgh, UK
[3] Department of Physics and Astronomy, Sonoma State University, Rohnert Park, USA
[4] Max-Planck-Institut fur extraterrestrische Physik, Garching, Germany
[5] The School of Physics and Astronomy, University of Nottingham, UK
[6] Kapteyn Astronomical Institute, University of Groningen, the Netherlands
[7] Spitzer Science Center, California Institute of Technology, Pasadena, USA
[8] Department of Physics and Astronomy, University of California, Irvine, USA
[9] CEA-Saclay/DSM/DAPNIA/Service d'Astrophysique, Gif-sur-Yvette, France
[10] National Optical Astronomy Observatories, Tucson, USA
[11] UCO/Lick Observatory, Department of Astronomy and Astrophysics, University of California, Santa Cruz, USA
[12] Harvard–Smithsonian Center for Astrophysics, Cambridge, USA
[13] Space Telescope Science Institute, Baltimore, USA
[14] Department of Astronomy, University of Massachusetts, Amherst, USA
[15] Aix–Marseille Université, CNRS, Laboratoire d'Astrophysique de Marseille UMR 7326, Marseille, France
[16] INAF–Osservatorio Astronomico di Trieste, Italy
[17] Max Planck Institute for Astronomy, Heidelberg, Germany
[18] INAF–Osservatorio Astronomico di Padova, Italy
[19] Minnesota Institute of Astrophysics and School of Physics and Astronomy, University of Minnesota, Minneapolis, USA
[20] INAF–Osservatorio Astronomico di Bologna, Italy
[21] Department of Astronomy, Steward Observatory, University of Arizona, Tucson, USA
[22] School of Physics and Astronomy, University of St. Andrews, United Kingdom
[23] Department of Physics and Astronomy, University of Missouri, Columbia, USA
[24] INAF–Osservatorio Astrofisico di Arcetri, Firenze, Italy

A new ultra-deep near-infrared imaging survey has been completed using the HAWK-I imager at the VLT. It is named HUGS (HAWK-I Ultra Deep Survey and GOODS Survey) and delivers the deepest, highest quality images ever collected in the *K*-band. HUGS complements the data delivered by the HST CANDELS survey over two well-studied extragalactic fields, and promises to open up exciting new opportunities to explore the highest redshift Universe. The survey is outlined and faint galaxy number counts and the search for passive galaxies in the early Universe are highlighted. The HUGS data have been completely analysed and are being made public to the worldwide community.

Why HUGS: The general context

Ultra-deep imaging surveys are of fundamental importance for advancing our knowledge of the early phases of galaxy formation and evolution. In general, each technological advance in telescopes and/or detectors has been swiftly applied to obtain ever deeper images of the extragalactic sky over a range of wavelengths. An obvious example of this technology-driven progress is the early Hubble Deep Field (HDF) campaigns (in the north, HDFN, and the south, HDFS) which have paved the way for the subsequent exploration of the high-redshift Universe. Building on the experience of these surveys, the concepts of colour-selection criteria and photometric redshifts have become commonly used tools in the exploration of galaxies at high redshifts. ESO has been major player in this field, as witnessed by various surveys like the New Technology Telescope (NTT) Deep Field (Fontana et al., 2000), the Very Large Telescope (VLT) FORS Deep Field (Heidt et al., 2003), the VLT-HDFS campaign (Fontana et al., 1999) and the near-infrared (NIR) coverage of the GOODS-South field (Retzlaff et al., 2010).

In recent years, the emphasis has started to shift progressively towards undertaking deep imaging surveys in the NIR, motivated by the need to sample the restframe optical (and even ultraviolet [UV]) emission in highly-redshifted galaxies in the young Universe. The most recent and spectacular case is the long series of Hubble Ultra Deep Field (HUDF) campaigns (Illingworth et al., 2013 and references therein), obtained with the infrared channel of the Wide Field Camera 3 (WFC3/IR), the latest and most efficient instrument on board the Hubble Space Telescope (HST).

The CANDELS survey (PI: S. Faber, Co-PI: H. Ferguson) is the latest, and most ambitious enterprise of this kind. CANDELS is a 900-orbit HST Multi-Cycle Treasury (MCT) programme delivering 0.18-arcsecond J_{F125W} and H_{F160W} images reaching ≈ 27.2 (AB mag; 5σ) over

0.25 square degrees, with even deeper (≈ 28 AB mag; 5σ) three-band (*Y*, *J*, *H*) images over ≈ 120 square arcminutes (within GOODS-South and GOODS-North). It also delivers the necessary deep optical HST Advanced Camera for Surveys (ACS) parallels to complement the deep WFC3/IR imaging.

The major scientific goals of the CANDELS MCT programme are: the assembly of statistically useful samples of galaxies at $6 < z < 9$; the measurement of the morphology and internal colour structure of galaxies at $z = 2–3$; the detection and follow-up of supernovae at $z > 2$ for validating their use as cosmological distance indicators; and the study of the growth of black holes in the centres of high-redshift galaxies.

As soon as CANDELS was approved, it was immediately realised that the addition of an adequately deep *K*-band coverage of the CANDELS fields might significantly expand the scientific exploitation of this wonderful dataset. It is worth remembering that, at $z = 6$, the wavelength gap between *H*-band and 3.6 μm is comparable to the gap between the observed *Z*- and *K*-bands at $z = 3$. Thus, bridging this large spectral range with deep *K*-band photometry is crucial for an accurate determination of the restframe physical quantities (e.g., stellar age, stellar mass and dust content) of galaxies at very high redshifts.

The scientific goals of HUGS

To fill this gap, we decided to undertake an ambitious programme designed to make optimum use of the most advanced NIR imager available at any current ground-based telescope: HAWK-I (the High Acuity Wide field *K*-band Imager; Kissler-Patig et al., 2008) at the VLT. On account of its unprecedented combination of depth and area coverage, HAWK-I is the ideal choice to deliver the ultra-deep and wide *K*-band images that are needed over the CANDELS field.

Although HUGS is designed to complement the WFC3 CANDELS observations, it is a free-standing survey that will enable independent scientific investigations, thanks to the depth of the *K*-band images.

The *K*-band is indeed considered an excellent proxy for the selection of mass-selected samples of galaxies at high redshift (Fontana et al., 2006). A primary goal of HUGS is hence the measurement of the evolution of the galaxy mass function at high redshift, especially at the faint end where *K*-band selected samples are required to be as complete in mass as possible. As another example, the wavelength shift from the H_{F160W} band (the longest accessible with HST) to the *K*-band enables us to extend the redshift coverage of the restframe *B*-band from $z \approx 2.6$ to $z \approx 4$. This will allow analysis of the restframe optical morphology and spectral energy distribution of $z \approx 4$ galaxies.

The data

The HUGS survey has been executed over the last three years as an ESO Large Programme (186.A-0898, PI: A. Fontana). It consisted of 208 hours of observations with HAWK-I, mostly in the *K*-band. The final HUGS dataset includes also all the previous imaging programmes that have been executed with HAWK-I in recent years over the GOODS-South field, both in the *Y*-band and *K*-band. These are an earlier Large Programme designed to select $z \approx 7$ galaxies (181.A0717, P.I. Fontana; see Castellano et al., 2010) as well as early HAWK-I Science Verification data (60.A-9284). Our survey targets two of the three CANDELS fields accessible from Paranal, namely GOODS-South and the UKIRT Infrared Red Deep Sky Survey (UKIDSS) Ultra-Deep Survey (UDS), since the ongoing UltraVISTA survey is already delivering ultra-deep *Y*-, *J*-, *H*- and *K*-band imaging within the COSMOS CANDELS field.

The depth of the images in the *K*-band has been tuned in order to match the depth of the WFC3/IR images produced in the J_{F125W} and H_{F160W} filters. In practice, the target depth was chosen to be 0.5 mag shallower than obtained with WFC3/IR in H_{F160W}, as appropriate to match the average (*H* - *K*) colour of faint galaxies.

The pointing strategy is also designed to best cover the CANDELS fields. In the UDS field, three different pointings are able to cover 85 % of the field, with a small overlap that has been used to cross-check photometric calibration. The coverage of the GOODS-South field with CANDELS is more complex, and forced us to adopt a more complicated pattern for the HUGS observations. The WFC3 observations are deeper in a rectangular region at the centre, where the HUDF is also located, and shallower in the upper

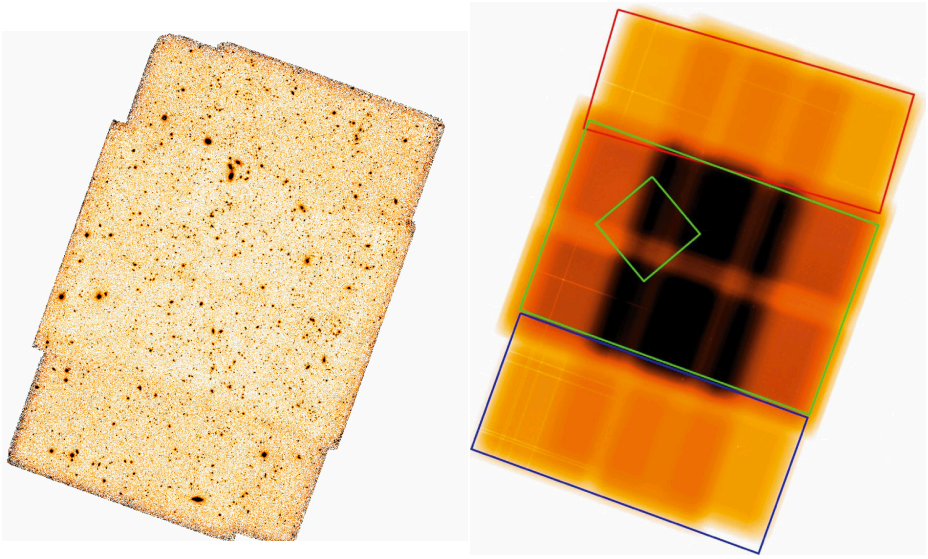

Figure 1. The final HUGS image of the GOODS-South field, in the *K*-band is shown (left image). On the right, the exposure map is shown: darker regions correspond to longer exposure. Overlaid are also the main WFC3 regions: CANDELS-deep (large green rectangle), CANDELS-wide (blue rectangle), Early Release Science (ERS as red rectangle) and HUDF (smaller green box).

and lower part of the field. We have therefore adopted a 2 × 3 grid of pointings, with significant overlaps. The resulting image is shown in Figure 1, including the position of the six individual pointings overlaid upon the WFC3 exposure map (that also includes the position of the HUDF and the other parallel deep fields) as well as the final exposure map.

It is immediately appreciated that the coverage of the GOODS-Deep area is not uniform, because of the combined effects of the pointing locations and the HAWK-I gaps. It reaches about 85 hours of net exposure time in the most central area that covers most of the HUDF, and still reaches more than 40 hours of exposure time over the remaining part of the GOODS-Deep area.

All the data have been collected and analysed. We initially used two pipelines (one developed in Rome and one in Edinburgh) to independently reduce the images acquired in the first year of observations. We then compared the two pipelines and the resulting reduced images: the two results agreed very well and this comparison was utilised to help yield a final, optimised version of the Rome pipeline that has been used in the final processing of all the data. We eventually cross-checked the relative calibration, not only internally (in the regions where the different pointings overlap), but also against wider area but shallower surveys (obtained with UKIDSS or the SOFI instrument), finding that images are calibrated at the 1–2 % level.

Final images and catalogues

The final quality of the output data is simply spectacular, and shows that HAWK-I on the VLT is capable of approaching HST's performance, even in the case of NIR deep imaging where HST is unrivalled. In the *K*-band the seeing is exceptional and homogeneous across the various pointings, confined to the range 0.38–0.43 arcseconds, the former value holding in particular in the ultra-deep area with 85 hours of exposure. In this deepest region (which includes most of the HUDF) we reach a 1σ magnitude limit per square arcsecond of ≈ 28.0 AB mag. In the UDS field the survey is about one magnitude shallower (to match the correspondingly shallower depth of the CANDELS images), but also includes *Y*-band imaging, which also has an excellent seeing between 0.45 and 0.5 arcseconds. A summary of the final quality of the data is presented in Table 1.

A visual comparison of the WFC3/IR and HAWK-I data is offered in Figure 2, where we compare the deepest region from HUGS and CANDELS. It can be immediately appreciated that the depth and quality of the HUGS images is comparable in all aspects to the WFC3 data.

In addition to final images, we have also obtained high-quality photometric catalogues in both areas. These have been obtained using the WFC3 *H*-band image from CANDELS as the detection image, and HUGS magnitudes have been obtained using a point spread function (PSF) matched photometry technique that takes into account the morphology of each object during the deblending process. The photometry was accomplished using the TFIT package (Laidler et al., 2007).

It may be of some interest to use these catalogues to show how effective the HUGS images are in providing us with useful information on the CANDELS-detected objects, since that is one of the main aims of the HUGS survey. In the case of GOODS-S, it is seen that as much as 90 % of the *H*-band detected galaxies have some flux measured at signal-to-noise (S/N) > 1 in the *K*-band, down to the faintest limits of the *H*-band catalogue, and that nearly 50 % of the $H \approx 26$ galaxies (and 15 % of the $H \approx 27$ galaxies) have a solid *K*-band detection with S/N > 5. As a practical example, we show in Figure 3 the spectral energy dis-

Table 1. Summary of HUGS observations for the various pointings.

Field	Band	Exposure time	Seeing (arcsec)	Lim. mag (AB, 1σ arcsec^{-2})
GOODS-DEEP1,2	*K* (2.2 μm)	31.5 hours	0.38–0.39	27.8
GOODS-WIDE1,2,3,4	*K* (2.2 μm)	11.3–13 hours	0.38–0.42	27.3–27.4
UDS1,2,3	*K* (2.2 μm)	12.5–13.5 hours	0.37–0.43	27.3–27.4
UDS1,2,3	*Y* (0.98 μm)	8 hours	0.45–0.5	28.2–28.4

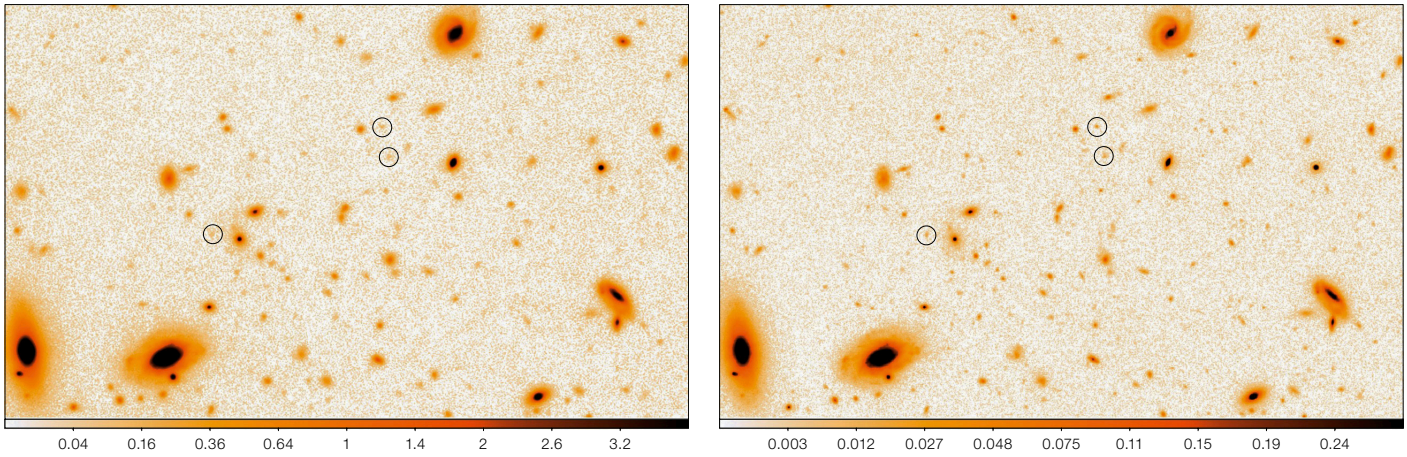

Figure 2. The centre of the deepest GOODS-S field as observed with HAWK-I is shown in the *K*-band (left) and with WFC3/IR in the *H*-band (right). The displayed area is 1 arcminute wide. Objects encircled have $H \approx 26$ mag and a colour $(H - K) \approx 0.5$, typical of faint galaxies.

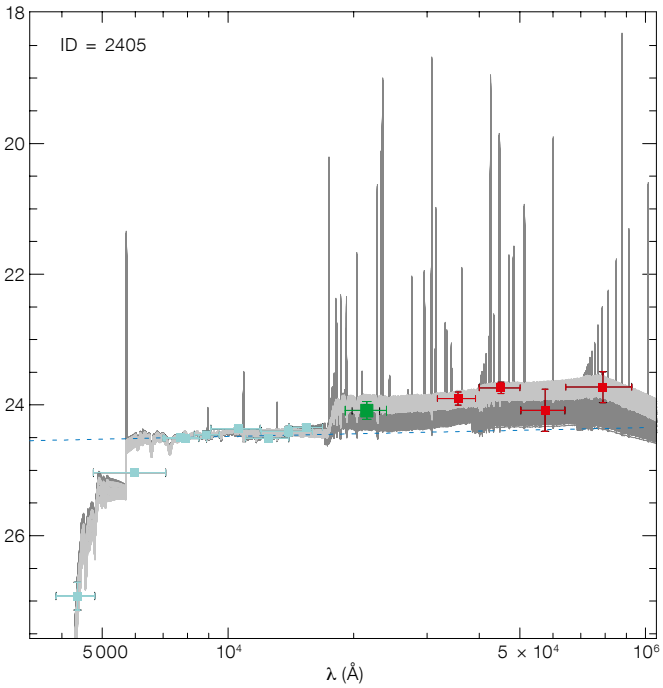

Figure 3. Spectral energy distribution of a galaxy at spectroscopic redshift $z \approx 3.7$, among the highest-redshift galaxies with measured metallicity (Castellano et al., 2014). The magnitudes (in the AB system) are $H \approx 24.3$ and $K \approx 24$. Cyan points represent photometric measures from HST; the green point from the HUGS *K*-band; red points are Spitzer data. Spectral fits in light grey are best fitting Bruzual and Charlot (2003) models with no nebular emission lines; fits in dark grey are Bruzual and Charlot models with nebular emission included.

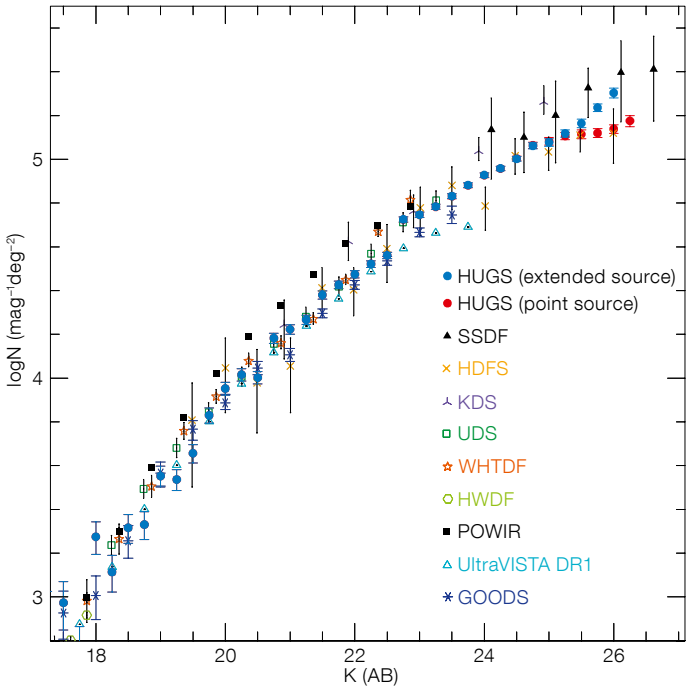

Figure 4. The *K*-band galaxy number counts derived from the HUGS survey, corrected for incompleteness and other systematic effects as described in the text. HUGS points in blue have been corrected for incompleteness with point sources; those in red by extended sources. Data from other deep surveys are also included.

tribution of a galaxy at spectroscopic redshift $z \approx 3.7$ in the GOODS-South field (adapted from Castellano et al., 2014). It is clearly seen that the HAWK-I band data is crucial to sample, at high S/N, the region immediately long-ward of the Balmer break. A full analysis of this and other $z \approx 3$ galaxies can be found in Castellano et al. (2014).

The faintest galaxies as observed in the *K*-band

An immediate glimpse of the scientific merit of a deep field is the derivation of the number counts. In the *K*-band, these are scientifically important since it has been claimed that the total extragalactic background light (EBL), as measured by satellite observations, exceeds the integrated contribution of observed galaxies, if the number counts are as shallow as those obtained by the deepest available observations so far (Subaru Super Deep Field [SSDF]: Minowa et al., 2005). These galaxy number counts have been computed from adaptive-optics-assisted Subaru observations on quite a small field (1 × 1 arcminute). If confirmed, this would imply the existence of some exotic population of primeval galaxies that appear at very faint fluxes.

The HUGS observations reach the same depth as the Subaru observations, but over a much larger area, and are hence perfectly suited to address this issue. Number counts have been derived independently from each pointing on both UDS and GOODS-S images, and a weighted average of these has then been used to obtain the final number counts. After trimming the outer regions of the images, the final area over which we compute the number counts is 340.58 square arcminutes, i.e. about 1/10th of a square degree. However, the deepest number counts (i.e., those determined at $K > 25$) are in practice determined from a sub-area of 50.17 square arcminutes within the GOODS-S field.

Central to a robust determination of the number counts is a thorough and reliable estimate of the incompleteness and other systematics, which must be obtained through the use of simulations. The estimate of the size and magnitude dependence of the correction depends on a critical assumption, namely the distribution of galaxy sizes. At the exquisite resolution of the HUGS images the difference between compact and point-like sources is indeed measurable. We therefore computed the correction for incompleteness in two cases: i) assuming point-like sources; and ii) assuming a distribution in size between 0.1 and 0.3 arcseconds, the typical size that we measure in the *H*-band HST images. The derived number counts are shown in Figure 4, for both assumptions about galaxy size (blue symbols for point sources, red for extended), compared with a number of recent results from the literature. As expected, the number counts agree very well with previous results from the literature. It is immediately appreciated that the HUGS number counts exceed in depth and statistical accuracy of all previous estimates at faint magnitudes, the only exception being the very faintest bin from the SSDF (Minowa et al., 2005).

At the faint limit, it is immediately clear how dramatic is the impact of the assumptions on galaxy size. Assuming point-like sources we confirm the flattening of the number counts at $K \approx 24$–26 reported by Minowa et al. (2005), in our case with a much larger statistical accuracy (due to the 50 times larger field of view of our images). However, assuming instead a more realistic, typical galaxy size in the range 0.1–0.3 arcseconds, we find that the slope of the number counts remains essentially unchanged up to $K \approx 26$, with a slope of about ≈ 0.18 (see Figure 4). If we assume that the steep slope that we find for resolved galaxies holds to even fainter limits, the consequence is that most of the diffuse EBL observed from space can be ascribed to ordinary galaxies, without the need to invoke more exotic populations.

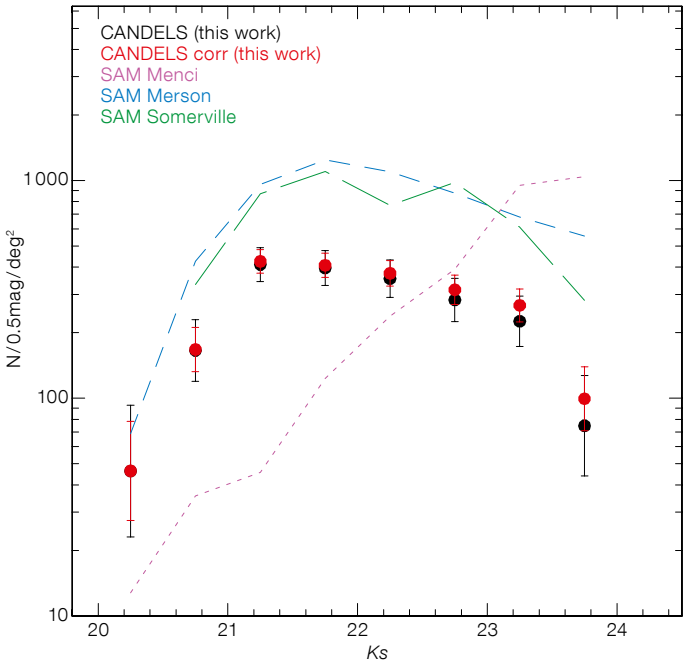

Figure 5. Number counts of passively evolving galaxies at $z \approx 2$ (black: raw counts, red: corrected for incompleteness), from the HUGS survey is illustrated. Comparison of the observed points to three different semi-analytic galaxy models (SAM) are shown.

Passive galaxies in the early Universe

Another early scientific result that we have obtained from these data, in conjunction with the other CANDELS data, is related to the study of passively evolving galaxies at $z \approx 2$. Adopting the *pBzK* criterion proposed by Daddi et al. (2004) to identify such objects, and thanks to the unprecedented depth of our observations, we have now extended the selection of these objects at magnitudes ($K \approx 25$), fainter than was possible in any previous analysis. We have demonstrated for the first time through simulations that we can select passive galaxies down to $K \approx 24$ without being significantly affected by incompleteness, and that the latter is still treatable down to $K \approx 25$.

Our central result (shown in Figure 5) is that the *pBzK* number counts show a flattening at $K \approx 21$, and a turn-over at $K \geq 22$, equivalent to restframe absolute *I*-band magnitudes of $M_I = -23$ and -22 respectively. Converted into stellar mass, our result corresponds to a decrease in the number density of passive-evolving galaxies at stellar masses below $10^{10.8}\ M_\odot$ for a Salpeter initial mass function. As judged against the still steeply rising number counts of the overall galaxy population at these redshifts, this turnover is fairly abrupt, indicating that at high redshift the mechanism that quenches star formation activity is much less efficient below this mass limit.

Comparing our observed number counts with a population of quiescent galaxies extracted from three different theoretical models of galaxy formation, we find that only two of these models reproduce even qualitatively the observed trend in the number counts, and that none of the models provides a statistically acceptable description of the number density of quiescent galaxies at these redshifts. This result clearly shows that the mass and luminosity distribution of quiescent galaxies at high redshift continues to present a key and demanding challenge for proposed models of galaxy formation and evolution. Full details are given in a dedicated paper (Sommariva et al., 2014).

A wealth of data made public

We are fully aware that the data described here may have a much larger impact if the whole astronomical community is allowed access to them. The survey strategy and all the details of data reduction and the number counts are presented in Fontana et al. (2014). All the data from the HUGS survey are available in various forms — as images for individual pointings, as images of full mosaics, as well as multi-wavelength catalogues. Data are available from the ASTRODEEP website[1] as well as from the ESO archive as Phase 3 data products[2]. We look forward to the science that will be possible with this wonderful dataset.

References

Bruzual, G. & Charlot, S. 2003, MNRAS, 344, 1000
Castellano, M. et al. 2010, A&A, 511, A20
Castellano, M. et al. 2014, A&A, in press, arXiv:1403.0743
Daddi, E. et al. 2004, ApJ, 617, 746
Fontana, A. et al. 1999, A&A, 343, 19
Fontana, A. et al. 2000, AJ, 120, 2206
Fontana, A. et al. 2006, A&A, 459, 745
Fontana, A. et al. 2014, A&A, in press
Heidt, J. et al. 2003, A&A, 398, 49
Kissler-Patig, M. et al. 2008, A&A, 491, 941
Illingworth, G. D. et al. 2013, ApJS, 209, 6
Laidler, V. G. et al. 2007, PASP, 119, 1325
Menci, N. et al. 2005, ApJ, 632, 49
Merson, A. I. et al. 2012, arXiv:1206.4049
Retzlaff, J. et al. 2010, A&A, 511, A50
Somerville, R. S. et al. 2012, MNRAS, 423, 1992
Sommariva, V. et al. 2014, A&A, submitted

Links

[1] ASTRODEEP website: www.astrodeep.eu
[2] ESO Phase 3 products: https://www.eso.org/sci/observing/phase3.html